ISBN: 978-3-95450-247-9 ISSN: 2673-5490 doi: 10.18429/JACoW-IPAC2024-MOPS42

START-TO-END SIMULATIONS OF MICROBUNCHING INSTABILITY BASED ON OPTIMIZED VELOCITY BUNCHING IN LINAC-DRIVEN FELS

W. C. Cheng[1], Z. H. Zhu[1], M. H. Zhao
Shanghai Institute of Applied Physics, Chinese Academy of Sciences, Shanghai, China
M. Zhang*, D. Gu
Shanghai Advanced Research Institute, Chinese Academy of Sciences, Shanghai, China
[1]also at University of Chinese Academy of Sciences, Beijing, China

Abstract

The microbunching instability (MBI) driven by beam collective effects can cause significant electron beam quality degradation in advanced X-ray free electron lasers. Typically, multiple stage magnetic bunch compressors used to generate high peak current electron beam will dramatically amplify the microbunching instability. In this paper, by redesigning the solenoid elaborately and adopting a dual-mode buncher cavity with the third harmonic mode used to correct the RF curvature, in combination with the evolutionary many-objective beam dynamics optimization, it is potential for the electron beam to be further compressed in velocity bunching (VB) process. Therefore, a VB plus one bunch compressor could be a promising alternative scheme to achieve moderate peak current beam for X-ray FELs. Start-to-end simulations based on the Shanghai high-repetition-rate XFEL and extreme light facility proves the feasibility of the scheme in suppressing the additional MBI gain due to multi-stage magnetic bunch compressors.

INTRODUCTION

The microbunching instability driven by beam collective effects degrades the electron beam quality significantly in linacs for advanced X-ray FELs [1–5]. Typically, two stage or multiple stage magnetic bunch compressors are used to provide high peak current electron beam. However, Magnetic bunch compressor (BC) inherently amplifies the microbunching instability due to coherent synchrotron radiation (CSR) [6] and longitudinal space charge (LSC) [7].A natural idea to restrain the microbunching gain is to use one stage magnetic BC, but there will be more pressure to maintain stability against timing jitter and peak current jitter [8]. Alternatively, a hybrid mode based on Velocity bunching plus one BC scheme may be a promising method to suppress the microbunching instability [9, 10]. The effectiveness of this scheme to adequately suppress MBI in the short wavelength region was demonstrated by theoretical calculations in a previous study [10].

However, since VB operates in the ultra-low energy phase, the strong space charge force will result in a large emittance growth and the nonlinear beam longitudinal phase space distortion. Preliminary optimisations were carried out based on the injector parameters of the Shanghai High-Repetition-Rate XFEL and Extreme Light Facility (SHINE) [10]. In this paper, with further optimisation based on a multi-objective genetic algorithm NSGA-II [11], the electron beam with peak current of 45 A and transverse emittance of only 0.3 mm·mrad was introduced at the injector exit. Therefore, electron beam with a peak current of 1500 A can be obtained in the SHINE linear accelerator by only switching on the second stage of the magnetic compressor (BC2).

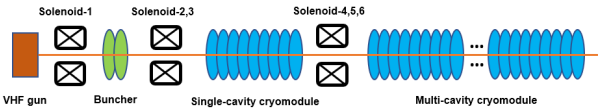

Figure 1: The schematic layout of the optimized SHINE injector section.

Comparison of the theoretical MBI gain for the hybrid mode ('VB+BC') scheme with the normal two-stage compression scheme ('VB+2BC') shows the potential of the former in suppressing the microbunching instability at short-wavelength region [10]. The MBI gain of SHINE from the injector to the linear accelerator was simulated by adding an initial sinusoidal density modulation to the driven laser, and the simulation results were in agree with the theoretical analysis illustrating the effectiveness of the hybrid mode scheme.

DYNAMICS OPTIMIZATION IN VB

The method based on velocity bunching was proposed to increase the peak current of electron beam more than two decades ago [12]. The principles of VB have been demonstrated in previous study with detailed formula derivation [9]. Indeed, by properly choosing the injection phase and the acceleration gradient, the electron beam can be compressed in VB process.

Shanghai High-Repetition-Rate XFEL and Extreme Light Facility (SHINE), which is the first high-repetition-rate hard X-ray FEL facility based on superconducting linac in China, is being constructed. The schematic layout of photoinjector is shown in Fig. 1. The 216.7 MHz VHF gun is followed by the buncher, the single and eight 9-cell superconducting cryomodules. The transverse emittance growth is controlled by the six sets of solenoids are placed along the beamline.

The NSGA-II genetic algorithm has been applied by researchers in the accelerator system dynamics optimisation process due to its efficiency and effectiveness. In the dynamics optimisation of VB of the SHINE injector, the optimi-

* zhangmeng@sari.ac.cn

ISBN: 978-3-95450-247-9 ISSN: 2673-5490 doi: 10.18429/JACoW-IPAC2024-MOPS42

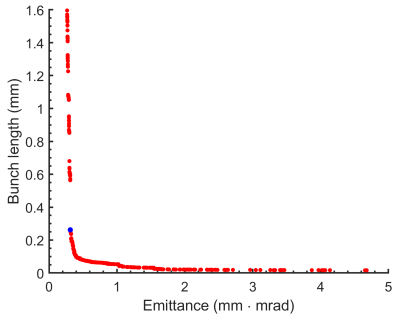

Figure 2: Map of the Pareto frontier in the last generation, where the blue dots indicate the optimal solution chosen.

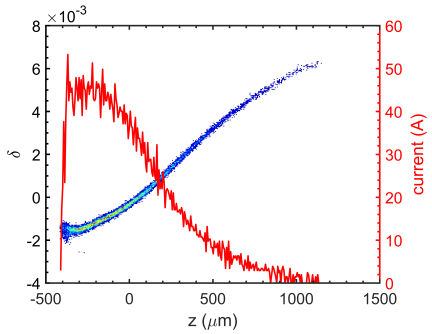

Figure 3: Simulation results of longitudinal phase space and current profile of the electron beam with optimal solution parameters selected from the Pareto front.

sation objectives are short beam length and low transverse emittance. There are a total of 20 optimisation variables in the optimisation process, including the RF phase and amplitude of each cavity, as well as the magnetic field strength and position of the six sets of solenoids. To ensure convergence of the final optimisation results, the generation population size was set to 400 and iterated 200 times to depict the optimal Pareto front for electron beam length and transverse emittance. Pareto frontier optimisation results are shown in Fig. 2. There is an obvious negative correlation between the electron beam length and the transverse emittance. In Fig. 2, the lower left region is the optimal solution region, and the solutions for each parameter in this region were simulated using ASTRA [13], and finally the blue dot was chosen as the optimal solution parameter, corresponding to an electron beam length of 0.2622 mm and a transverse emittance of only 0.3127 mm·mrad.

Based on the injector layout and parameters corresponding to the blue dots in Fig. 2 simulated using ASTRA, the longitudinal phase space and current distribution of the beam at the injector outlet are shown in Fig. 3, and the beam current can be up to 45 A. Therefore, electron beam with a peak current of 1500 A can be obtained in the SHINE linear accelerator by only switching on the second stage of the magnetic compressor, the scheme being abbreviated as 'VB+1BC'. The layout of the SHINE linear accelerator 'VB+1BC' and 'VB+2BC' schemes is shown in Fig. 4. Figure 4(b) shows

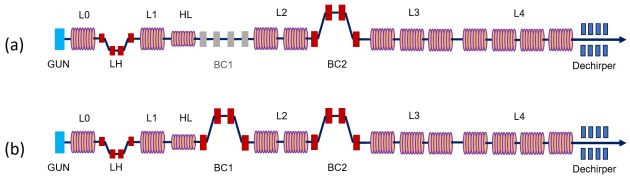

Figure 4: Schematic layout of the SHINE linear accelerator 'VB+1BC' (a) and 'VB+2BC' (b).

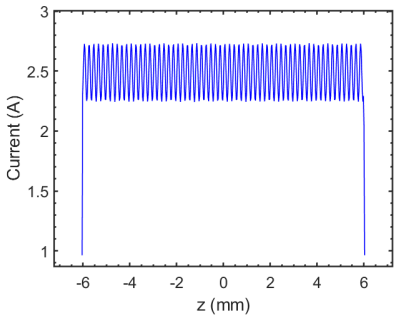

Figure 5: Initial current distribution with cosine modulation at the cathode. The average current of the beam is 2.5 A, modulation wavelength $\lambda = 200\,\mu$m, modulation amplitude $A = 10\,\%$.

the layout of the SHINE injector and the linear accelerator with normal parameters, denoted as the 'VB+2BC' scheme.

SIMULATION VERIFICATION OF MBI FROM INJECTOR TO LINAC AT SHINE

Previous study [10] has demonstrated by theoretical derivation that the "VB+1BC" scheme has a greater potential for suppressing microbunching instability in the short-wavelength modulation region than the "VB+2BC" scheme. In this section, beam dynamics simulations based on ASTRA and Elegant are carried out for the SHINE injector and linac so as to validate the results of previous theoretical derivations.

Initial Modulation Generation for Simulation at SHINE Injector

Supposing a beam at the cathode with an initial current of I_0 with a small cosine perturbation, it can be expressed as $I(z) = I_0(1 + A\cos kz)$, where k is the modulation wave number, A is the modulation amplitude. Sampling the above current distribution after dividing it into q grids along the longitudinal direction, its probability density function (PDF) can be described as

$$p(z) = (1 + A\cos kz)/q\ , \qquad (1)$$

where q should be much larger than the modulation period. For a beam with N particles, each parid needs to be filled with $Np(z)$ particles according to the above equation, so that the initial modulated beam at the cathode for simulation can be generated, which is shown as Fig. 5. The beam has an average current of 2.5 A, a density modulation wavelength

ISBN: 978-3-95450-247-9 ISSN: 2673-5490 doi: 10.18429/JACoW-IPAC2024-MOPS42

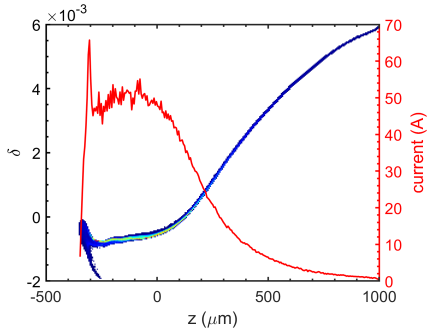

Figure 6: Simulation results of the longitudinal phase space and current profile (red line) of the electron beam at the exit of the SHINE injector for 'VB+1BC' scheme.

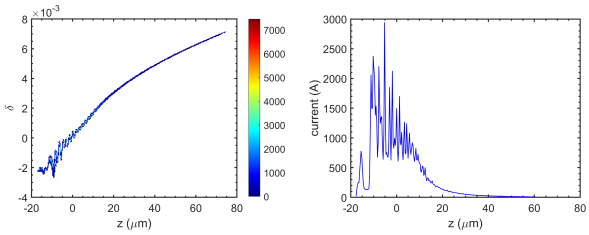

(a) (b)

Figure 7: Simulation results of the longitudinal phase space (a) and current profile (b) of the electron beam at the exit of the SHINE L4 for 'VB+1BC' scheme.

of $\lambda = 200\,\mu$m, and a modulation amplitude of $A = 10\,\%$. Based on optimised injector parameters by NSGA-II and ASTRA, the beam longitudinal phase space and current distribution at the exit of injector is shown in Fig. 6. The smearing of the density modulation is mainly from the strong plasma oscillation because beam energy is relatively low [9].

Simulation at SHINE Linac

For the 'VB+1BC' scheme layout of the SHINE linac, the beam longitudinal phase space and current distribution at the exit of L4 is shown in Fig. 7. The burr structure caused by the microbunching instability can be seen in the beam current distribution.

To characterize the microbunching instability in the simulation, we introduced the concept of bunching factor as:

$$b(k) = \frac{1}{N}\sum e^{-ikz_i} \,. \tag{2}$$

The corresponding bunchingfactors of the beam at the cathode and L4 exit are shown in Fig. 8. The max bunchingfactor at the exit of L4 is 0.092. Therefore, a beam with an initial modulation wavelength of $\lambda = 200\mu$m has an MBI gain of $G_{\lambda_0=200} \approx 0.092/0.1 = 0.92$.

In order to compare with the theoretical MBI gain of the "VB+1BC" scheme calculated in the study [10], we use the same method mentioned above with initial modulation of $\lambda = 200\,\mu$m to simulate and validate the MBI gain of $\lambda = 500\,\mu$m, 700 μm, 1000 μm, 1200 μm. The comparison of the final simulated and theoretical MBI gains is shown in

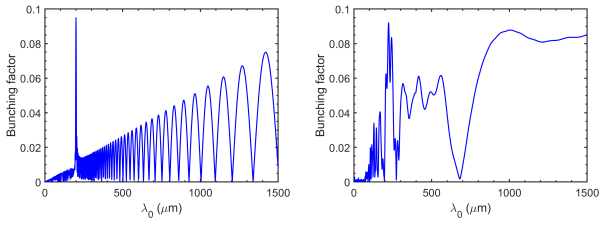

(a) (b)

Figure 8: The bunching factor corresponding to the initial modulation wavelength $\lambda_0 = 200\,\mu$m: (a) at initial position, and (b) at the exit of L4.

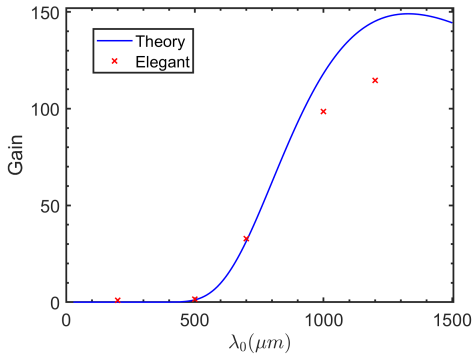

Figure 9: Comparison of simulated and theoretical MBI gain curve, where λ_0 is the initial modulation wavelength.

Fig. 9. From the figure, it can be seen that the simulation results of the MBI gain based on Elegant converge with the theory in the short modulation wavelength region, and only slightly smaller than the theoretical value in the long wavelength region.

CONCLUSION

In this paper, the beam dynamics of the velocity compression process of the SHINE injector is optimised based on NSGA-II. The MBI theoretical derivation in the previous study is validated by the start-to-end simulation. It is demonstrated that the 'VB+1BC' scheme is feasible to suppress the microbuching gain at short-wavelength region.

REFERENCES

[1] M. Borland *et al.*, "Start-to-end simulation of self-amplified spontaneous emission free electron lasers from the gun through the undulator", *Nuclear Instruments and Methods in Physics Research Section A: Accelerators, Spectrometers, Detectors and Associated Equipment*, vol. 483, no. 1, pp. 268–272, 2002. doi:10.1016/S0168-9002(02)00325-X

[2] Z. Huang *et al.*, "Suppression of microbunching instability in the linac coherent light source", *Phys. Rev. ST Accel. Beams*, vol. 7, p. 074401, Jul 2004. doi:10.1103/PhysRevSTAB.7.074401

[3] M. Venturini, "Microbunching instability in single-pass systems using a direct two-dimensional Vlasov solver", *Physical Review Special Topics - Accelerators and Beams*, vol. 10,

ISBN: 978-3-95450-247-9 ISSN: 2673-5490 doi: 10.18429/JACoW-IPAC2024-MOPS42

no. 10, pp. 1–10, 2007. doi:10.1103/PhysRevSTAB.10.104401

[4] M. Borland, "Modeling of the microbunching instability", *Phys. Rev. ST Accel. Beams*, vol. 11, p. 030701, Mar 2008. doi:10.1103/PhysRevSTAB.11.030701

[5] Z. Huang and G. Stupakov, "Control and application of beam microbunching in high brightness linac-driven free electron lasers", *Nuclear Instruments and Methods in Physics Research Section A: Accelerators, Spectrometers, Detectors and Associated Equipment*, vol. 907, pp. 182–187, 2018. doi:10.1016/j.nima.2018.02.030

[6] Z. Huang, M. Borland, P. Emma, and K. J. Kim, "Theory and simulation of CSR microbunching in bunch compressors", *Nuclear Instruments and Methods in Physics Research, Section A: Accelerators, Spectrometers, Detectors and Associated Equipment*, vol. 507, no. 1-2, pp. 318–322, 2003. doi:10.1016/S0168-9002(03)00937-9

[7] E. Saldin, E. Schneidmiller, and M. Yurkov, "Longitudinal space charge-driven microbunching instability in the tesla test facility linac", *Nuclear Instruments and Methods in Physics Research Section A: Accelerators, Spectrometers, Detectors and Associated Equipment*, vol. 528, no. 1, pp. 355–359, 2004. doi:10.1016/j.nima.2004.04.067

[8] M. Cornacchia *et al.*,"Running fermi with one-stage compressor: advantages, layout, performance", LBNL Technical Note *LBNL-62765*, 2008

[9] D. Xiang and J. Wu, "Microbunching instability in velocity bunching", SLAC Technical Note SLAC-PUB-13646, 2009.

[10] W. Cheng, Z. Zhu, M. Zhao, M. Zhang, and D. Gu, "Suppression of Microbunching Instability based on optimized velocity bunching in linac-driven FELs", *J. Phys.: Conf. Ser. 2687 062016*, 01 2024. doi:10.1088/1742-6596/2687/6/062016

[11] K. Deb, A. Pratap, and S. Agarwal, "A fast and elitist multiobjective genetic algorithm: NSGA-II", *IEEE Transactions on Evolutionary Computation*, 2002, 6(2):182-197. doi:10.1109/4235.996017

[12] L. Serafini and M. Ferrario, "Velocity bunching in photo-injectors", in *AIP conference proceedings*, vol. 581, no. 1, pp. 87–106, 2001. doi:10.1063/1.1401564

[13] K. Floettmann, ASTRA, https://www.desy.de/~mpyflo/